International Journal of Heat and Mass Transfer 62 (2013) 178–183

Contents lists available at SciVerse ScienceDirect

International Journal of Heat and Mass Transfer

journal homepage: www.elsevier.com/locate/ijhmt

Technical Note

A large scale Titanium Thermal Ground Plane

Marin Sigurdson *, YuWei Liu, Payam Bozorgi, David Bothman, Noel MacDonald, Carl Meinhart

Mechanical Engineering Department, University of California Santa Barbara, Santa Barbara, CA 93106-5070, United States

ARTICLE INFO

Article history:
Received 29 June 2012
Received in revised form 22 January 2013
Accepted 23 January 2013
Available online 25 March 2013

Keywords:
Heat pipe
Grooved wick
Titanium
Capillary pressure

ABSTRACT

A thermal ground plane, flat heat pipe (30 cm × 7.6 cm × 4.5 mm thick) was developed as a passive heat spreading component for electronics cooling. The combination of multiscale titanium wick fabrication with laser welding results in an all-titanium device which is light (500 g) yet strong, hermetically sealed, and compatible with water. Numerical simulations were used to optimize the grooved wick design by minimizing viscous drag present in any large scale heat pipe, while maintaining sufficient capillary force. Nanoporous titania coats the grooved wick to further enhance wettability. The resulting heat pipe was tested on two different test configurations, and is capable of a maximum heat flow rate in vertical (reflux) orientation of 500 W for chip temperatures of 100 °C, and 1000 W for chip temperatures of 150 °C. This translates into a maximum effective thermal conductivity of ~8000 W/m K. Such a high thermal conductivity indicates that the Titanium Thermal Ground Plane is an effective heat pipe, and when combined with a heat sink, useful for cooling an array of electronic components.

1. Introduction

Thermal management of electronic components is becoming increasingly critical as transistor density and power density of integrated circuits increases. Heat pipes are commonly used to transport heat in electronic components. Commercially available heat pipes are commonly of the copper-tube format [1]. These are inexpensive, and very successful in some markets, particular in cooling graphics cards or GPU's for gaming applications, where heat from a chip needs to be dispersed locally. When scaled up in length and power, many copper tube heat pipes can lose efficiency. As the transport distance increases, viscous drag of the wick – which is sintered copper or copper mesh – will ultimately become sufficiently large and dramatically decrease mass flow rate. To address increasingly high heat and heat flux requirements, researchers have investigated heat pipe improvements such as loop heat pipes [2,3], enhanced conductivity nanofluids [4], and arrays of embedded miniature heat pipes [5–8]. Heat pipes with nanofluids use working fluids seeded with nanoparticles to increase fluid conductivity, and have been shown to improve greatly heat pipe performance. Miniature heat pipes use an array of small diameter heat pipes or channels in a flat format and can move high heat flux of 140 W/cm^2 [8,9] over short distances (12 cm total length). However, for large distances, miniature heat pipes may lose efficiency due to viscous drag.

Nanoporous coating of micro-wick structure is also of interest in heat pipe enhancement. It has been shown, both theoretically and experimentally, that a porous coating on groove structures improves heat transfer coefficient through improved evaporation [10–12]. Wang and Catton for example, find the heat transfer rate due to evaporation in triangular grooves to be 3–6 times greater when coated with a thin porous layer. A nanostructured titania (termed NST) coating for titanium TGP is incorporated in the heat pipe reported in the current manuscript.

2. Device design

The Ti-TGP, or Titanium Thermal Ground Plane was developed in response to the need for a large format, thin, flat heat pipe, or a Thermal Ground Plane, optimized for moving large amounts of heat from mounted chips to a distantly located heat sink. In the Ti-TGP, we addressed this challenge by (1) using a multiscale wick for the best balance of capillary force and viscous drag, and (2) optimizing wick geometry through numerical simulation. Traditional copper heat pipes are heavy, limited in power capability, and, due to the tube shape and thermal mismatch issues, difficult to mount efficiently on semiconductor chips. The Ti-TGP addresses these problems with a thin, flat format with a relatively compliant mounting surface, light yet strong case material (titanium), and heat load design optimized through numerical simulations. A small scale (3 cm × 3 cm) Ti-TGP was developed first, and proved our Ti-multiscale wick concept, with effective thermal conductivity

* Corresponding author.
E-mail addresses: marin@engineering.ucsb.edu (M. Sigurdson), yuwei@engineering.ucsb.edu (Y. Liu), payam@engineering.ucsb.edu (P. Bozorgi), bothman@engineering.ucsb.edu (D. Bothman), nmacd@engineering.ucsb.edu (N. MacDonald), microfluid@gmail.com (C. Meinhart).

0017-9310/$ - see front matter © 2013 Published by Elsevier Ltd.
http://dx.doi.org/10.1016/j.ijheatmasstransfer.2013.01.064

Nomenclature

A	cross sectional area of wick (m)
A_{TGP}	cross sectional area of Ti-TGP (m)
d	distance between grooves (m)
g	groove width (m)
g_x	gravity component in streamwise direction (m s^{-2})
h_g	vapor chamber depth (m)
h_f	groove depth (m)
h_{fg}	latent heat of vaporization (J kg^{-1})
k	thermal conductivity (W m^{-1} K^{-1})
K	wick permeability (m^2)
L	wick length (m)
ΔP_{cap}	capillary pressure (Pa)
Q	heat flow rate (W)
R_c	thermal contact resistance (W K^{-1})
T	temperature (°C or K)
w	wick width (m)

Greek symbols

γ	surface tension (N m^{-1})
μ	viscosity (Pa s)
ρ	density (kg m^{-3})

Subscripts

v, g	vapor
f, l	liquid
eff	effective

k_{eff} = 350 W/m K [13]. The current Ti-TGP required several changes in design, dimensions and processing to accommodate the larger size (8 cm × 40 cm); as a result it is not only more versatile, but offers much better performance.

The TGP is intended to operate either flat, or in reflux orientation (vertical; hot side down), and weight should be minimized. Heat flow rate should be maximized while keeping the chip temperature below about 100 °C. These requirements suggest a titanium-water heat pipe with custom designed grooved wick. A cross-sectional diagram of the final design is shown in Fig. 1; design considerations are detailed below.

2.1. Titanium design advantages

The low conductivity of titanium (k = 21 W/(m K)), compared with copper (k = 400 W/(m K)), can result in a high thermal resistance through the Ti-TGP case. This is mitigated however, by the high fracture toughness of titanium, which allows the case to be very thin without suffering mechanical failure. Additionally, for long heat pipes, R_{case} is of diminishing significance compared with the thermal resistance due to viscous drag. For large heat pipes, the attractive mechanical properties of titanium, such as the density to stiffness ratio, and fracture toughness, are increasingly important. Titanium heat pipes have been used previously in space applications, where weight is critical [9,14].

The multiscale fabrication capability of titanium is another attractive feature: it can be (1) macromachined using traditional machining processes, (2) microfabricated using micropatterned masks and wet or dry etching, and (3) hermetically laser welded [15,16]. Additional processing described in the following section can add a nanostructured coating to the wick. Titanium is highly compatible with water, which is the best working fluid for our applications. Titanium is therefore a well-suited material for heat pipes that require a cm to meter scale envelope, a μm to mm scale wick, with a nm scale porous coating.

2.2. Super-wetting surface: NST

Wettability of the titanium-water interface is an important factor in wicking velocity, which drives heat flow rate. To improve wettability, and decrease effective contact angle to near zero, a nanoscale super-wetting surface treatment was integrated with the wick design. We previously developed a process by which titanium can be oxidized with heated hydrogen peroxide to yield a highly porous surface we term Nano-Structured-Titania (NST) [17], with pore features on the order of 100 nm (Fig. 1). NST substantially improves wettability; we have shown that adding a NST coating to a microscale wick can increase wicking velocity by 70% [13]. Higher wicking velocity will lead to higher heat flow rate, and better performance. The porous coating is also expected to improve performance through improved evaporation, as previous work with porous coatings on grooved wicks demonstrated [10–12]. The integration of a semi-porous titania coating on a grooved titanium wick in a titanium envelope presents a elegant heat pipe that is potentially lightweight, strong, efficient, and long lasting.

2.3. Geometry and assembly

The Ti-TGP is designed in two titanium pieces: wick and backplane. The wick substrate is processed, first through etching to create the micro-scale wick structure, and then through NST process described above, to create nanoscale structure. The backplane with vapor chamber, mounting holes, and feed-through holes, are macro-machined. Wick and backplane are hermetically sealed together with pulsed laser welding. Modified titanium *Swagelok™* fittings are welded on access holes in the backplane for the purpose of fill ports. Although only one port is ultimately required, prototype designs included two ports for flexibility. Assembled device is shown in Fig. 2.

2.4. Wick design

The wick design is based on manufacturing constraints, simulation, and testing. It consists of a microscale groove structure overlaid with nanoporous titania (Fig. 1). For the small-scale Ti-TGP developed earlier, we used an array of pillars [13,17,18], but for this large-scale heat pipe, grooves were chosen. In this section, we optimize microscale groove dimensions g (groove width), h_f (groove depth) and d (distance between grooves) in a wick of length L and width w.

The purpose of the wick is to return liquid from the condenser to the evaporator through capillary force (and gravitational force, in reflux orientation) and against viscous drag. In order to discover the optimum geometry to balance these forces and yield highest heat flow rate, and with foundation from [18] and [6], we developed a model to balance capillary pressure drop with pressure drop due to viscous drag, and maximize heat flux (details in supplementary material):

$$\dot{Q}_{heat,max} = \frac{2wh_{fg}\lfloor \Delta P_{cap}/L + (\rho_f - \rho_g)g_x \rfloor}{(\mu_f/\rho_f h_f K + 12\mu_g/\rho_g h_g^3)} \quad (1)$$

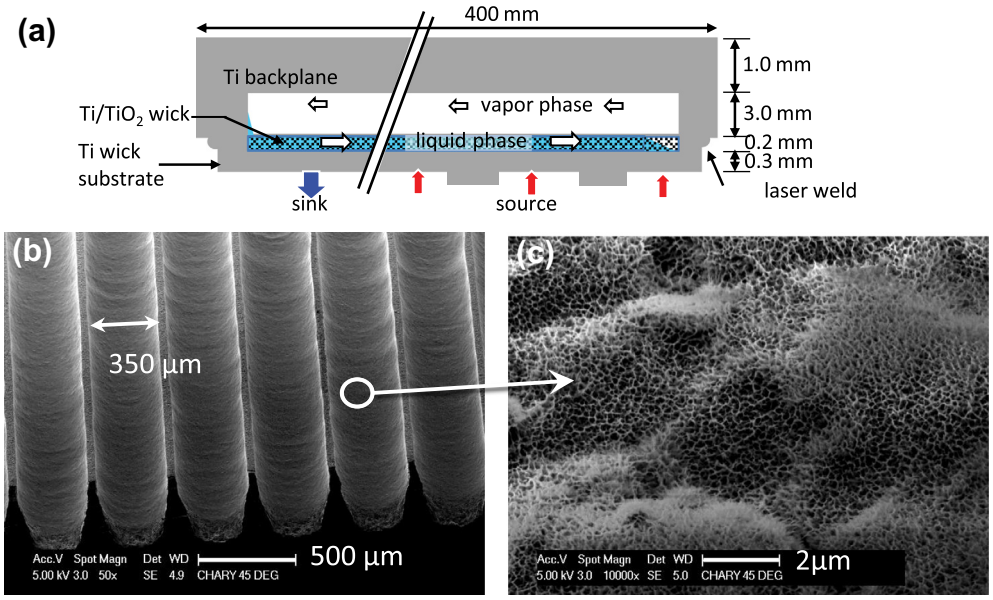

Fig. 1. Cross sectional diagram of Ti-TGP design (not to scale; center section omitted). The Ti wick substrate with etched wick is laser welded to the Ti backplane, with recessed vapor chamber. A heat sink can then be mounted to the left hand side (condenser region) while heat sources are mounted between strengthening ribs in the evaporator region. Under operation, water fills the wick, evaporating above the heat sources, and condensing at the heat sink. SEM of multiscale Ti/TiO_2 wick, cut to show cross sectional profile. Etched grooves in Titanium substrate are 250 µm deep × 350 µm wide. The etch process creates surface roughness (visible striations) on the order of 1–5 µm. (c) The titanium is oxidized to produce the NST structure, which has features on the order of 100 nm. This creates a super-hydrophobic surface, which improves the wetting characteristics of the wick structure.

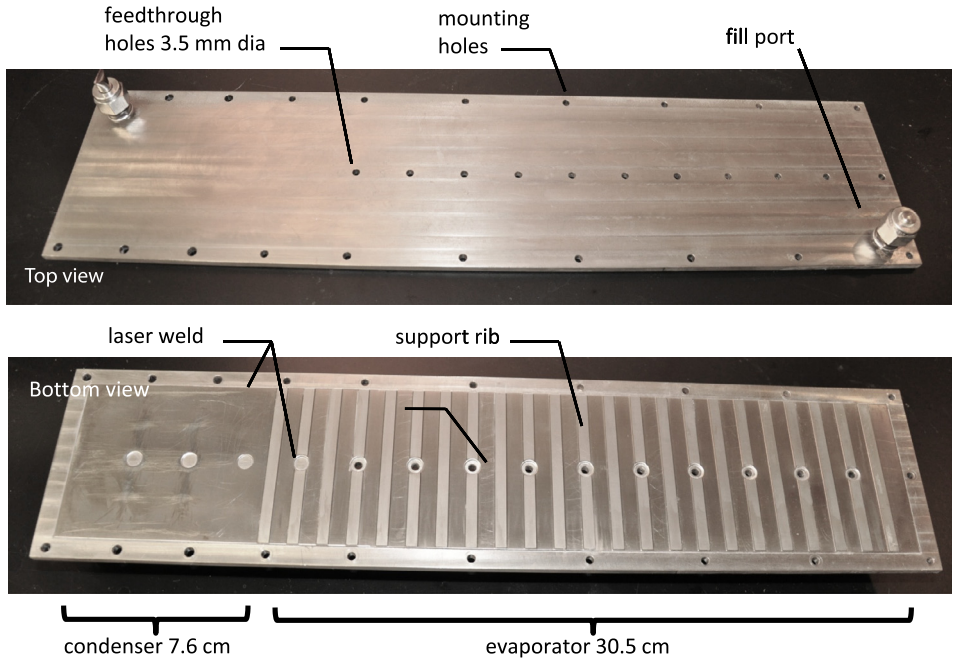

Fig. 2. Ti-TGP, top and bottom views. The TGP was constructed by laser-welding the wick (bottom view) to a machined backplane with vapor cavity (top view). The backplane has two fill-ports, mounting holes around the edge, and feed-through holes for electrical access through the center. Bottom view shows support ribs to prevent bowing under vacuum, and feed-throughs in evaporator section, which are replaced with solid welded posts in condenser section. Heaters or chips will be mounted between support ribs.

where h_{fg} is the latent heat; ρ_f, ρ_g, μ_f, and μ_g are the liquid and gas densities and viscosities; and gx is gravity. The wick permeability is

$$K = \frac{1}{2h_f^2(g+d)}\left\{\sum_{n=0}^{\infty}\frac{1}{\lambda_n^5}\left[\lambda_n g - \sinh\lambda_n g - \left(\frac{1-\cosh\lambda_n g}{\sinh\lambda_n g}\right)(\cosh\lambda_n g - 1)\right]\right\} \quad (2)$$

where $\lambda_n = (2n+1)\pi/2h_f$, $n > 1$. We use liquid and vapor properties at 60 °C; $g_x = 0$ (horizontal orientation); and $h_f = 200$ µm (reasonable maximum etch depth for our current process). We then can then optimize wick dimensions d and g by calculating maximum heat flow rate for: 50 µm $\leqslant d \leqslant$ 500 µm and 50 µm $\leqslant g \leqslant$ 500 µm. These ranges were constrained based on microfabrication capability. Fig. 3 shows contours of maximum heat transfer rate for this parameter space. Therefore, to obtain the greatest heat transfer rate in horizontal orientation, we use $h_f = 200$ µm, $g = 350$ µm, $d = 50$ µm for the groove geometry, which gives a maximum heat flow rate of

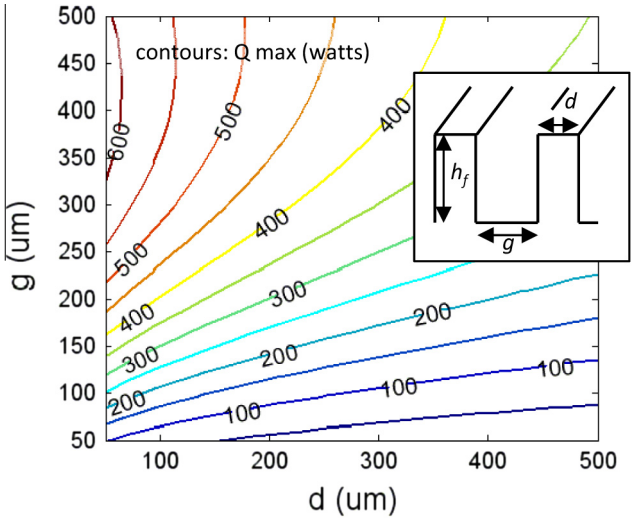

Fig. 3. Numerical simulation results: level curves of maximum heat transfer Q_{max} as a result of the capillary limit, for operation in the horizontal orientation. Results are plotted for 200 μm groove height, which yields much higher heat flux than 100 μm groove height (not shown). These results, as well as fabrication limitations, resulted in wick design parameters h = 200 μm, g = 350 μm, d = 50 μm. Inset shows groove parameter nomenclature.

500 W. In the reflux (vertical) orientation, capillary pressure is less important, and maximum heat flow rate increases steadily with gap, with less dependence on groove separation, d. With the same groove dimensions, in the vertical orientation, the maximum heat flow rate is estimated to be $Q_{max,capillary}$ = 6000 W. From analysis of entrainment, boiling, and sonic limit (supplementary material), we expect the heat flow rate to be limited by capillary pressure in horizontal operation, and by entrainment in vertical operation.

2.5. Charging

The TGP charging station was designed to allow precise filling of the TGP with optimum water volume such that at the target operating temperature, there is sufficient liquid volume to wet the wick. This is difficult to calculate *a priori* due to the variable meniscus in groove, and to areas with unpredictable flooding or dryout, such as fill ports, or internal support structures. The fill volume was therefore optimized via trial and error. It is also essential to avoid introduction of any noncondensible gasses, as they will partially block the TGP operation and result in lower heat flow rate. The TGP charging manifold was designed to minimize noncondensible gas by incorporating water-degas cycles, and pre-fill evacuation of the TGP. The TGP is evacuated to 4 mTorr prior to filling; deionized water is degassed through three freeze-pump-thaw cycles. The water is forced into a graduated burette through a combination of pressure and temperature differentials, and then a precise volume is bled into the TGP.

A custom copper-nickel fill tube was swaged to a modified titanium *Swagelok*^{TM} fitting welded to the TGP. The pinched seal, and the entire TGP are hermetic; weight of the TGP has not decreased over 3 months of moderate testing. An initial fill volume of 5.2 mL resulted in premature dryout, and so the device was recharged with a fill volume of 7.2 mL, resulting in better performance. Future optimization of fill volume may further improve performance.

3. Thermal test setup

The Ti-TGP was tested at UCSB and at an independent testing facility located at the Army Research Laboratory (ARL) in Adelphi MD. The UCSB test setup (Fig. 4) was designed to approximate operating conditions, with accommodations for budget, versatility, and extra diagnostics. For example, only 8 of the 24 mounting strips were used. Each mounting strip is designed to accommodate a row of IC's, but in the UCSB test set, a cartridge heater embedded in an aluminum heater block is used instead. Thermocouples embedded in the block allow heat flow rate monitoring. Cooling was supplied by a laboratory water chiller in combination with a 4-pass cold plate, interfaced to the Ti-TGP via a 76 mm × 76 mm × 6 mm copper block.

Thermal paste (Arctic Silver 5) was used at all interfaces between the TGP and the test set. The thermal resistance at the interface was estimated using manufacturer's data for thermal conductivity (k = 8.7 W/m K) and an estimated effective contact layer thickness t = 500 μm. The contact resistance was estimated $Rc = t/k \approx 500$ m^{2}K/W. Although this order of magnitude estimate was confirmed through testing of a metal plate of known thermal conductivity, tests also demonstrated Rc can change by a factor of 10 or more with slight adjustments in mounting. In particular, because the wick was somewhat flexible, the degree of contact between the TGP and the test set increased with TGP internal pressure, which increased with temperature. As a result, it was difficult to determine contact resistance accurately.

Thermocouple temperatures were acquired using a *National Instruments* data acquisition platform (compact DAQ), and recorded via a *Labview* program every 10 s. Cooling water remained constant temperature through each test, while heater voltage was incrementally increased. Each data point shown below was taken after test set and TGP had reached steady temperature, after 10–15 min.

4. Results & discussion

4.1. Thermodynamic diagnostics: vapor temperature

Under ideal conditions, a heat pipe contains only liquid and vapor water under saturated conditions, where the pressure and temperature are related by the water saturation curve. Internal pressure variations vary slightly due to viscous drag and capillary pressure, and are small compared with the internal thermodynamic pressure. If the internal pressure is approximately uniform, then the adiabatic region of the TGP will be isothermal The TGP vapor temperature is estimated by measuring the case temperature using thermocouples fastened to the top surface of the TGP.

The results for operation in flat orientation (Fig 5) indicate that the temperature profile is approximately isothermal along the length of the TGP, except at the extreme edges. Temperature at the coldest end of the condenser is lower. This may be due to an accumulation of noncondensible gas (NCG), which is not constrained to the saturation temperature, but can range between the condenser and vapor temperatures. The temperature drop at the distal end of the condenser is much smaller for higher vapor temperature. This is presumably because lower temperature results in lower thermodynamic internal pressure, allowing the NCG to expand in the condenser end. Heat transfer is minimal where NCGs flood the condenser surface, and so the NCG and the TGP top surface above it, are colder. An improved method for eliminating NCGs would be advantageous. The evaporator temperature at the edge of the TGP for the highest heat flow rate, 220 W, indicates dryout, and the presence of super-heated steam. In this case, the capillary pressure of the wick was not sufficient to overcome viscous pressure drop. These vapor temperature measurements along the heat pipe allow confirmation of saturation conditions, and a diagnostic tool for the Ti-TGP.

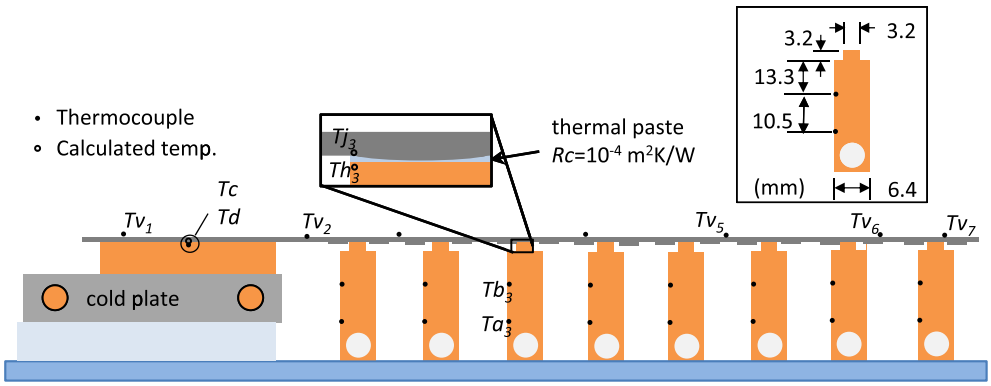

Fig. 4. UCSB test set thermocouple (TC) position and nomenclature. TC's Tv_{1-7} are taped to the top of the TGP; Heater thermocouples (Ta, Tb) are glued in holes drilled into the heater risers. The riser top temperature Tj_i is calculated based on extrapolation from the riser thermocouples Ta_i, Tb_i. TGP junction temperature Th_i is then calculated assuming a thermal paste contact resistance.

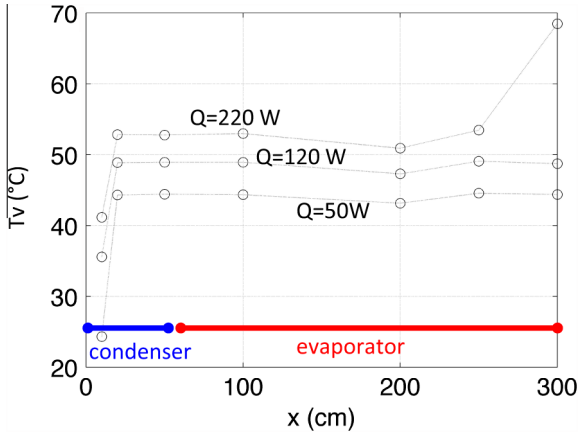

Fig. 5. Vapor temperature along the length of the Ti-TGP, in the 0° (flat) orientation. Temperature drop at cold end is much more pronounced than in the previous figure, as volume of noncondensible gas is larger at lower temperature and pressure. At 220 W, the temperature of the evaporator end rises steeply, indicating dryout.

4.2. Performance metric: thermal conductivity

Although the Ti-TGP cannot strictly be evaluated using thermal conductivity, because the temperature profile is not linear, for comparison purposes, it is helpful to define an "effective" thermal conductivity:

$$k_{eff} = QL_{eff}/(T_{hot} - T_{cold})A_{TGP}, \quad (3)$$

Q is heat flow rate, approximated with electrical power; L_{eff} is effective length (19 cm), T_{hot} and T_{cold} are evaporator and condenser characteristic temperatures and A_{TGP} is the cross-sectional area of the TGP.

Thermal conductivities of the Ti-TGP were measured in both test sets in the vertical orientation, assuming zero or finite contact resistance, and are shown in Fig. 6. Effective thermal conductivity ranges from about 3000 to 8000 W/m K, depending on the applied power, and contact resistance assumptions, for the heat flow rate range 300 W < Q < 1200 W. This emphasizes the fact that effective thermal conductivity cannot be a universal standard measurement for heat pipes, as it is for homogeneous materials. Nevertheless, we can understand some important trends. For low heat flow rate, the Ti-TGP is less efficient at moving heat, resulting from the lower vapor mass density associated with lower vapor temperature, and that noncondensible gas occupies a larger volume of the vapor chamber. Performance can also decrease if the heat flow rate is too high, due to local wick dryout.

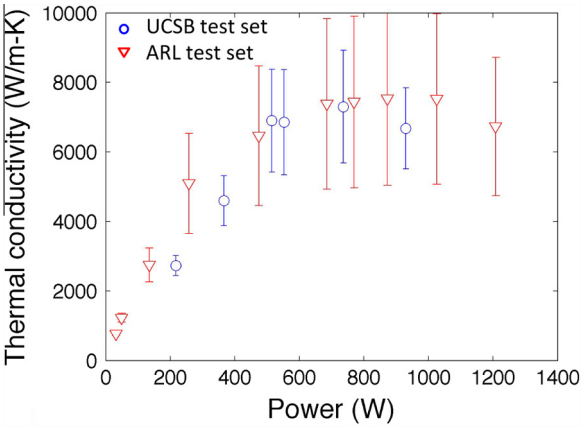

Fig. 6. Effective thermal conductivity assuming an empirically derived contact resistance ($Rc = 5 \times 10^3$W/K). Lower error bar extends to $Rc = 0$; upper error bars extend to $Rc = 7.5 \times 10^3$W/K. We conservatively estimate the effective conductivity lies in this range.

5. Conclusions

We have developed a titanium-based flat heat pipe, Ti-TGP, that measures 40 cm long × 7.6 cm wide × 5 mm thick, weighs 500 g, with an effective thermal conductivity of $k = 5000$–8000 W/m K. When combined with a cooler such as a high efficiency heat sink, the Ti-TGP is capable of removing up to $Q = 1$ kW of power from mounted chips, or about $Q = 500$ W of power if chip surface temperature is limited to 100 °C. The titanium material is well suited for many heat pipe applications, because it has a high strength-to-weight ratio, high fracture toughness, corrosive resistant in harsh conditions, and is highly compatible with water. In addition, it is the only material that can be microfabricated, macro-machined, and hermetically welded. The titanium-based thermal ground planes are applicable to high-performance applications, where large scale, lightweight, and high performance thin, flat thermal ground planes are important.

Acknowledgements

This work was supported by DARPA grant W31P4Q-10-1-0010. The authors would like to acknowledge Alex Colbourn (UCSB); Darin Sharar, Nicholas Jankowski, and Brian Morgan (ARL) for help testing the Ti-TGP.

Appendix A. Supplementary data

Supplementary data associated with this article can be found, in the online version, at http://dx.doi.org/10.1016/j.ijheatmasstransfer.2013.01.064.

References

[1] L. Shang, R.P. Dick, Thermal crisis: challenges and potential solutions, IEEE Potentials 25 (5) (2006) 31–35.
[2] A. Ambirajan, A.A. Adoni, J.S. Vaidya, A.A. Rajendran, D. Kumar, P. Dutta, Loop heat pipes: a review of fundamentals, Oper. Des. Heat Transfer Eng. 33 (4–5) (2011) 387–405.
[3] L. Vasiliev, D. Lossouarn, C. Romestant, et al., Loop heat pipe for cooling of high-power electronic components, Int. J. Heat Mass Transfer 52 (1–2) (2009) 301–308.
[4] S.-W. Kang, W.-C. Wei, S.-H. Tsai, C.-C. Huang, Experimental investigation of nanofluids on sintered heat pipe thermal performance, Appl. Therm. Eng. 29 (5–6) (2009) 973–979.
[5] M.C. Zaghdoudi, S. Maalej, J. Mansouri, M.B.H. Sassi, Flat miniature heat pipes for electronics cooling: state of the art, experimental and theoretical analysis, World Acad. Sci. Eng. Technol. 75 (2011) 880–903.
[6] K.H. Do, S.J. Kim, S.V. Garimella, A mathematical model for analyzing the thermal characteristics of a flat micro heat pipe with a grooved wick, Int. J. Heat Mass Transfer 51 (19–20) (2008) 4637–4650.
[7] R. Hopkins, A. Faghri, D. Krustalev, Flat miniature heat pipes with micro capillary grooves, J. Heat Transfer 121 (1) (1999) 102–109.
[8] L. Lin, R. Ponnappan, J. Leland, High performance miniature heat pipe, Int. J. Heat Mass Transfer 45 (15) (2002) 3131–3142.
[9] X. Yang, Y.Y. Yan, D. Mullen, Recent developments of lightweight, high performance heat pipes, Appl. Therm. Eng. 33 (C) (2012) 1–14.
[10] J. Wang, I. Catton, Enhanced evaporation heat transfer in triangular grooves covered with a thin fine porous layer, Appl. Therm. Eng. 21 (17) (2001) 1721–1737.
[11] T. Semenic, I. Catton, Experimental study of biporous wicks for high heat flux applications, Int. J. Heat Mass Transfer 52 (21) (2009) 5113–5121.
[12] L.L. Vasiliev, L. Grakovich, M.I. Rabetskii, L. Vasiliev Jr., Grooved heat pipe evaporators with porous coating, in: Presented at the 16th International Heat Pipe Conference, Lyon, France, 2012, pp. 1–6.
[13] C. Ding, G. Soni, P. Bozorgi, B.D. Piorek, C.D. Meinhart, N.C. MacDonald, A flat heat pipe architecture based on nanostructured titania, J. Microelectromech. Syst. 19 (4) (2010) 878–884.
[14] Q. Baojin, Z. Li, X. Hong, S. Yan, Heat transfer characteristics of titanium/water two-phase closed thermosyphon, Energy Convers. Manage. 50 (9) (2009) 2174–2179.
[15] M.F. Aimi, M.P. Rao, N.C. MacDonald, A.S. Zuruzi, D.P. Bothman, High aspect ratio bulk micromachining of titanium, Nat. Mater. 3 (2004) 103–105.
[16] Z. Samah B. Butler, E. Parker, A. Ahmed, H. Evans, C. Safinya, N. MacDonald, Integrating Biomaterials into Microsystems: Formation and Characterization of Nanostructured Titania, Paper presented at: Mat. Res. Soc. Symp., 2004.
[17] P. Bozorgi, Application of YAG Laser Micro-Welding in MEMS Packaging, Nanotech 2010: Electronics, Devices, Fabrication, MEMS, Fluidics, and Computational, vol. 2, Nano Science and Technology Institute, 2010, pp. 5-8.
[18] N. Srivastava, C. Ding, A. Judson, N.C. MacDonald, C.D. Meinhart, A unified scaling model for flow through a lattice of microfabricated posts, Lab Chip 10 (9) (2010) 1148–1152.